Title	Wing base structure supports Coleorrhyncha + Auchenorrhyncha (Insecta: Hemiptera)
Author(s)	Yoshizawa, Kazunori; Ogawa, Naoki; Dietrich, Christopher H.
Citation	Journal of zoological systematics and evolutionary research, 55(3), 199-207 https://doi.org/10.1111/jzs.12173
Issue Date	2017-08
Doc URL	http://hdl.handle.net/2115/71153
Rights	This is the peer reviewed version of the following article: Journal of zoological systematics and evolutionary research, 55(3);p199-207, 2017 Aug, which has been published in final form at http://doi.org/10.1111/jzs.12173. This article may be used for non-commercial purposes in accordance with Wiley Terms and Conditions for Self-Archiving.
Type	article (author version)
File Information	2017JZS.pdf

1 Systematic Entomology, School of Agriculture, Hokkaido University, Sapporo 060-8589,

Japan; 2 Illinois Natural History Survey, University of Illinois, Champaign, Illinois 61820,

USA

Wing base structure supports Coleorrhyncha + Auchenorrhyncha (Insecta: Hemiptera)

Kazunori Yoshizawa 1, Naoki Ogawa 1 and Christopher H. Dietrich 2

Corresponding author: Kazunori Yoshizawa (psocid@res.agr.hokudai.ac.jp)

Contributing authors: Naoki Ogawa (ogawa222@res.agr.hokudai.ac.jp), Christopher H.

Dietrich (chdietri@illinois.edu)

13   **Abstract**

14

15   The phylogenetic placement of the moss bugs (Insecta: Hemiptera: Coleorrhyncha) has been

16   highly controversial. Many apparent morphological apomorphies support the close

17   relationship between Coleorrhyncha and Heteroptera (= true bugs). However, a recent

18   phylogenomic study strongly supported a sister-group relationship between Coleorrhyncha

19   and Auchenorrhyncha (planthoppers, leafhoppers, treehoppers, spittlebugs and cicadas). To

20   test these two alternative hypotheses, we examined the fore- and hindwing base structure of

21   the only known extant macropterous species of Coleorrhyncha using binocular and confocal

22   laser scanning microscopes and analyzed the data selected from the wing base

23   phylogenetically. When full morphological data including the wing base characters were

24   analyzed, the sister group relationship between Coleorrhyncha + Heteroptera was supported,

25   agreeing with previous consensus based on morphology. In contrast, when only wing base

26   characters were analyzed separately, the clade Coleorrhyncha + Auchenorrhyncha was

27   recovered, in agreement with the result from the phylogenomic study. The membranous

28   condition of the proximal median plate in the forewing was identified as a potential

29   synapomorphy of the latter grouping, and absence of the tegula was excluded as a potential

30   synapomorphy of Coleorrhyncha and Heteroptera.

31

32   **Key words:** Auchenorrhyncha – Coleorrhyncha – Heteroptera – phylogeny – wing base

33   structure

Introduction

The suborder Coleorrhyncha (moss bugs) is an enigmatic taxon of the order Hemiptera (Insecta). It consists of a single family, Peloridiidae, with fewer than 40 extant species restricted to circumantarctic regions (Burckhardt 2009; Burckhardt et al. 2011). With a combination of plesiomorphic and apomorphic features, the placement of this suborder within Hemiptera had been highly unstable. Traditionally, prior to explicit phylogenetic analyses of Hemiptera as a whole, Coleorrhyncha was regarded as a member of "Homoptera" (now generally regarded as a paraphyletic grade) due to presence of a complete tentorium, origin of the labium on the posteroventral portion of the head (and absence of a gula), discrete pro- and mesothracic ganglia, and eight pairs of abdominal spiracles, all of which are now regarded as plesiomorphies (Carver et al. 1991). In contrast, Coleorrhyncha share some apparent morphological apomorphies with Heteroptera (reviewed in Grimaldi and Engel 2005; Forero 2008; Burckhardt 2009), some of which have been controversial (e.g., Cobben 1978 but see also Schuh 1979). Recent extensive morphology-based cladistic analysis, with revised morphological observations including Coleorrhyncha, strongly supported Coleorrhyncha + Heteroptera (Friedemann et al. 2014). Multiple molecular phylogenetic studies based on 18S rRNA (Wheeler et al. 1993; Campbell et al. 1995; Ouvrard et al. 2000) and multiple gene regions (Cryan and Urban 2012) also provided support for this relationship. Therefore, until recently, available data appear to have converged toward consensus in support of the sister group relationship between Coleorrhyncha and Heteroptera (together referred to as Heteropterodea or Prosorrhyncha) (Grimaldi and Engel 2005; Forero 2008).

However, a recent phylogenomic study of Hexapoda that incorporated data from >1400 gene regions (Misof et al. 2014) casted doubt on this general view, placing Coleorrhyncha consistently as sister to Auchenorrhyncha (infraorder composed of planthoppers, leafhoppers, treehoppers, spittlebugs and cicadas). This result was supported by multiple datasets (i.e., nucleotide and amino acid sequences) and also received strong statistical support by bootstrapping and four-cluster likelihood mapping analyses (Misof et al. 2014, Supplement). The previously accepted sister group relationship between Coleorrhyncha and Heteroptera was also refuted by recent mitochondrial phylogenomic analyses (Cui et al. 2013; Wang et al. 2015). Therefore, an apparent conflict between morphological and molecular data has arisen in the placement of Coleorrhyncha.

66   The wing base structure comprises sclerites located between the insect thorax and

67   wing. This structure mediates the power produced by the thoracic indirect flight muscles to

68   the wings and also controls proper flapping and folding of the wings. Therefore, evolution of

69   this structure is strongly constrained and, thus, the wing base sclerites appear to evolve very

70   slowly (Hörnschemeyer 2002). Because of this unique property, the wing base structure has

71   previously been utilized for resolving controversial branches in hemipteroid phylogeny. For

72   example, although the monophyly of Auchenorrhyncha has been questioned based on

73   morphological (Bourgoin 1986ab 1993; Bourgoin and Huang 1990) and molecular criteria

74   (Campbell et al. 1995; Sorensen et al. 1995; Bourgoin et al. 1997; Ouvrard et al. 2000),

75   examination of wing base morphology provided unambiguous support for Auchenorrhyncha

76   (Yoshizawa and Saigusa 2001). Monophyly of Auchenorrhyncha subsequently received

77   strong support from the molecular phylogenetic (Urban and Cryan 2007; Cryan and Urban

78   2012) and phylogenomic (Misof et al. 2014) analyses, corroborating the value of wing base

79   structure for resolving difficult higher-level phylogenetic problems (see also Yoshizawa

80   2011).

81   In this study, we examined the morphology of the fore- and hindwing base structures

82   of a species of Coleorrhyncha, which were treated as missing characters by Friedemann et al.

83   (2014), to test the alternative hypotheses on the phylogenetic placement of this suborder.

84

85   **Material and Methods**

86

87   A dried specimen of *Peloridium hammoniorum* Breddin, 1897 collected in Chile in

88   2014 by CHD was used. This is the only extant species of Coleorrhyncha known to have

89   flight ability, although most individuals of this species have vestigial hindwings. The

90   individual studied possessed fully developed fore- and hindwings. The specimen was soaked

91   with 10% KOH at room temperature for one night. Later, the pterothorax was separated from

92   the other body parts, washed by distilled water, then 80% ethanol, and finally stored and

93   observed in glycerol.

94   Observations were made with an Olympus SZX 16 binocular microscope (Olympus

95   Co., Tokyo, Japan) and Leica TCS-SP5 Confocal Laser Scanning Microscope (CLSM)

96   (Leica Microsystems, Wetzlar, Germany). For binocular microscope observation, the

97   dissected specimen was pinned on a polyfoam using micro-pins, with the wings fully opened

98   but oriented in a slight downstroke position to observe all the sclerites in their natural shapes

99   dorsally. For CLSM imaging, specimens were mounted on a large cover glass (22 x 24 mm)

100   covered by a small cover glass (15 mm ø) to facilitate the observation of both dorsal and

101   ventral sides. We used an excitation wavelength of 488 nm and emission wavelength of 510–

102   680 nm. The emission waves were detected using two channels and visualized with two

103   pseudocolors (510–580 nm in green; 580–680 nm in red) (Mikó and Deans 2014). Homology

104   was assessed following Yoshizawa and Saigusa (2001), in which the criteria and landmarks

105   for homology identification of paraneopteran (hemipteroid) wing base sclerites were

106   explained. Terminology of Yoshizawa and Saigusa (2001) was also adopted.

107   Morphological data selected from the forewing base of *Peloridium* were newly

108   appended to two data matrices created previously: (1) the forewing base character matrix for

109   Paraneoptera, comprising 20 discrete characters, constructed by Yoshizawa and Saigusa

110   (2001), in which Coleorrhyncha was not examined; (2) the full morphological data,

111   comprising 119 characters (including the above as characters 20–39) compiled by

112   Friedemann et al. (2014), with some corrections to character coding as mentioned by

113   Yoshizawa and Lienhard (2016). The genus *Hackeriella* was used in the original full

114   morphological data matrix (Friedemann et al. 2014) but, because this genus lacks flight

115   ability, almost all wing base characters were previously coded as unknown. Here, the same

116   set of wing base characters scored for the separate wing base matrix was newly appended to

117   the matrix. Although this combination of data from two different peloridiid species created a

118   chimeric OTU in the data matrix, members of the family appear to be invariant for most (if

119   not all) of the included characters, so we would not anticipate a different phylogenetic result

120   had we scored all of Friedemann's characters for *Peloridium*. The hindwing base structure

121   was also observed but not included in the phylogenetic analyses to avoid the possibility of

122   over-weighting serially homologous (non-independent) traints, as discussed by Yoshizawa

123   and Saigusa (2001). Data matrices are available as online Supporting Information. The

124   datasets were analyzed by the maximum parsimony method using PAUP* 4a152 (Swofford

125   2002), with all characters weighted equally and branch-and-bound search performed. The

126   branch-and-bound method uses an exact algorithm that is guaranteed to find the most

127   parsimonious tree(s). Bootstrap and jackknife values were calculated using PAUP* with 1000

128   replicates (for jackknifing, version 4b10 was used because of problematic values provided by

129   4a152). For bootstrapping and jackknifing, heuristic searches with

130 tree-bisection-reconnection algorithm were performed, each with 100 replications and with

131 maxtrees = 10000. The decay index was calculated by using TreeRot V3 (Sorenson and

132 Franzosa 2007). The character state changes were calculated using MacClade 4 (Maddison

133 and Maddison 2001), and unambiguous character state changes were mapped onto the tree.

134

135 **Results**

136

137 *Forewing base morphology* (Fig. 1)

138   The anterior and median notal wing processes (ANWP and MNWP) are easily

139 identified as articular points with 1Ax: the former is well projecting but the latter is not. The

140 posterior notal wing process (PNWP) is less recognizable because it does not project and is

141 loosely associated with the third axillary sclerite. The tegula (Tg) is apparently present but

142 weakly sclerotized. The humeral plate (HP) is united with the basisubcostale (BSc). The

143 basiradiale (BR) is broadly united with BSc anteriorly, and is united with the second axillary

144 sclerite (2Ax) posteroproximally. The first axillary sclerite (1Ax) is subtriangular in shape

145 (see Fig. 1A; 1Ax is oriented laterally in Fig. 1B), lacking the anterior arm, with a weak

146 swelling on the proximal margin which articulates with MNWP. The anterior tip of 1Ax

147 articulates with the tip of BSc. The posteroproximal margin of 1Ax is also associated with the

148 notum. Distally, 1Ax articulates with 2Ax at two points; near the anterior tip and near the

149 posterodistal corner. 2Ax is subdivided into two sclerites, posteroproximal (pp) and

150 anterodistal (ad), clearly divided by a membranous region and the forked convex axillary fold

151 line. 2Ax-pp is tightly united with the apex of BSc anteroproximally and is articulated with

152 the well-developed and narrowly extended anterior arm of the third axillary sclerite (3Ax) at

153 its distal end. 2Ax-ad is united distally with the first distal median plate, and the convex

154 axillary fold line forms a border between the two sclerites. The proximal arm of 3Ax is

155 broadened and loosely articulated with the notum. Distally, it is tightly associated with the

156 basianal (BA) along the posterior margin (see Fig. 1A,C: in Fig. 1B, 3Ax and BA are

157 detached but this was caused artificially by slide mounting pressure). BA is well developed,

158 tightly articulated with the anal vein distally. The region corresponding to the proxomal

159 median plate (PMP) is completely membranous (see Fig. 1C). The distal median plate (DMP)

160 is subdivided into two elements. DMP1 is enlarged and convex dorsally. It is united

161 proximally with 2Ax, tightly associated with vein R anteriorly, and tightly articulated with

162 vein A posterodistally. DMP2 is located distal to DMP1, triangular in shape and very

163 narrowly extending toward the claval fold. The jugum (Jg) is apparently not developed.

164

165 *Hindwing base morphology* (Fig. 2)

166   [Note for CLSM image (Fig. 2B): Due to the less tight articulation of the hindwing

167 sclerites and pressure caused during slide mounting, the positions of many sclerites in the

168 CLSM image are distorted. See the line drawing (Fig. 2A) for their more natural articular

169 condition.]

170   ANWP and MNWP are recognizable but very loosely articulated with 1Ax, with the

171 former located anterior to the tip of 1Ax. PNWP is well developed and articulated with 3Ax.

172 Tg is absent. HP is united with BSc. BR is only recognizable as a small projection extending

173 from the posterior margin of BSc, and loosely associates with 2Ax at the tip. 1Ax is narrowed

174 over almost its entire length, only weakly broadened medially along the distal margin, with a

175 weakly developed anterior arm. The anterior tip of 1Ax only weakly articulates with the tip

176 of BSc. Distally, 1Ax articulates with 2Ax only at one point. 2Ax is not subdivided as in the

177 forewing but reduced in size and triangular in shape. It tightly articulates with 1Ax only at its

178 anteroproximal corner and also tightly articulates with 3Ax at its posterior tip. 3Ax is well

179 developed, rather loosely articulated with PNWP. Distally, it is tightly associated with the

180 anal vein (distal margin) and DMP (anterodistal corner). BA is indistinguishable from 3Ax.

181 The region corresponding to PMP is completely membranous. DMP is flat, trapezoidal in

182 shape. Jg is large but only weakly sclerotized.

183

184 *Phylogenetic analyses*

185   The parsimony analysis of the forewing base dataset resulted in only one most

186 parsimonious tree (Fig. 3: treelength = 23; consistency index = 0.91; retention index = 0.93).

187 This tree is completely congruent with that estimated by Yoshizawa and Saigusa (2001), with

188 monophyly of Paraneoptera, Condylognatha, and Hemiptera all supported. Coleorrhyncha

189 (excluded from the analysis of Yoshizawa and Saigusa 2001) formed a clade together with

190 the auchenorrhynchous infraorders (Cicadomorpha and Fulgoromorpha), supported by one

191 unique, non-homoplasious synapomorphy (decay index = 1): the membranous proximal

192 median plate (Character 13:1).

193   The parsimony analysis of the full morphology dataset, including the forewing base

194   characters, resulted in 18 equally parsimonious trees (treelength = 197; consistency index =

195   0.69; retention index = 0.85). Fig. 4 shows the strict consensus of 18 trees (differences

196   between them mostly concern the arrangements of zero-length branches and do not affect to

197   the following discussion: see Supporting Information for all trees). The tree is congruent with

198   that estimated by Friedemann et al. (2014), with Paraneoptera, Psocodea, Condylognatha,

199   Hemiptera, Auchenorrhyncha and Heteroptera supported as monophyletic. Coleorrhyncha

200   was placed as sister of Heteroptera, with three apomorphies (including two

201   non-homoplasious ones) supporting this placement. One of the characters selected from the

202   wing base (Character 28:1) provided non-homoplasious support for Hemiptera. The character

203   providing support for Auchenorrhyncha + Coleorrhyncha in the wing base dataset (Character

204   13:1 in the wing base matrix; 32:1 in the full data matrix) was only ambiguously

205   reconstructed: i.e., either independently evolved between Auchenorrhyncha and

206   Coleorrhyncha or gained in the common ancestor of Auchenorrhyncha + Coleorrhyncha +

207   Heteroptera but reversed in Heteroptera.

208

209   **Discussion**

210

211   The wing base structure in Coleorrhyncha largely retains the groundplan condition of

212   the neopteran wing base, except for the absence of a proximal median plate (Figs 1–2). All

213   modifications detected previously and thought to be autapomorphic for Hemiptera in general

214   (Yoshizawa and Saigusa 2001) were also observed in Coleorrhyncha. Overall, the wing base

215   structure of Coleorrhyncha resembles that of Auchenorrhyncha rather than Heteroptera

216   (Yoshizawa and Saigusa 2001; Yoshizawa and Wagatsuma 2012; Ogawa et al. 2015).

217   Maximum parsimony analysis of the wing base characters alone clearly supported the

218   monophyly of Coleorrhyncha + Auchenorrhyncha, with absence of PMP as a synapomorphy

219   (Fig. 3: decay index = 1, bootstrap/jackknife values = 67/51%). As mentioned by Yoshizawa

220   and Saigusa (2001), this is a "reduction" character, i.e., presumably resulting from the loss of

221   a sclerite, which may be regarded as less reliable than a character "gain". However, this

222   character state was previously regarded as an autapomorphy of Auchenorrhyncha, a group

223   once thought to be paraphyletic based on early single-gene molecular phylogenies (e.g.,

224   Campbell et al. 1995) but more recently supported as monophyletic by multi-gene molecular

225   phylogenies (Urban and Cryan 2007; Cryan and Urban 2012; Misof et al. 2014). In addition,

226   the present examination clearly identified the tegula on the forewing of Coleorrhyncha, which

227   invalidates "absence of tegula" as one of the previously proposed synapomorphies of

228   Coleorrhyncha + Heteroptera (Friedemann et al. 2014).

229   Nevertheless, analysis of the full morphological data still recovered the sister group

230   relationship between the Coleorrhyncha and Heteroptera (Fig 4: Friedemann et al. 2014),

231   although with lower support values (decay index = 1, bootstrap/jackknife values = 52/47%).

232   Synapomorphies supporting this relationship include presence of cephalic trichobothria

233   (54-1), tubular and four-segmented labium (56-2), and four-segmented flagellomeres (59-1).

234   The first two are non-homoplasious characters (Friedemann et al. 2014) in the present dataset.

235   The full morphological matrix constructed by Friedemann et al. (2014) lacked some

236   morphological characters previously suggested as additional synapomorphies of

237   Coleorrhyncha + Heteroptera (Grimaldi and Engel 2005; Forero 2008; Burckhardt 2009;

238   Spangenberg et al. 2013) so it is possible that morphological support for the monophyly of

239   this group is stronger than shown in our analysis.

240   In contrast, morphological support for the Coleorrhyncha + Heteroptera may not be as

241   robust as generally assumed. For example, the position of abdominal spiracle 2 on an

242   epipleurite was previously suggested as a potential synapomorphy of Coleorrhyncha and

243   Auchenorrhyncha (Sweet 1996). However, because almost all other morphological characters

244   supported a closer relationship between Coleorrhyncha and Heteroptera, Sweet (1996)

245   concluded that the spiracle condition was independently gained by Coleorrhyncha and

246   Auchenorrhyncha. The cephalic trichobothria (54-1) were scored as present for

247   Coleorrhyncha and Heteroptera (Friedmann et al. 2014) and identified as one of their

248   non-homoplasious synapomorphies (Fig. 3). However, the cephalic trichobothria were not

249   illustrated or reported in the recent detailed study of the adult head of *Hackeriella*

250   (Spangenberg et al. 2013) so the status of this character as a synapomorphy of Coleorrhyncha

251   + Heteroptera is questionable. Spangenberg et al. (2013) further reviewed morphological

252   evidence supporting the monophyly of Coleorrhyncha + Heteroptera but pointed out that the

253   homologies of some potential synapomorphies (e.g., the number of antennomeres) remain

254   uncertain while others (e.g., absence of cervical sclerites) are homoplasious. They also noted

255   several potential synapomorphies of Coleorrhyncha and Auchenorrhyncha, or Coleorrhyncha

256   and "Homoptera" in general. Some of the latter, including absence of a gula and presence of a

257   complete tentorium, were interpreted as plesiomorphic for Hemiptera as a whole, but

258 presence of Evans' organ (Bourgoin 1986b) may be another unique synapomorphy of

259 Coleorrhyncha and Auchenorrhyncha or an autapomorphy of "Homoptera" (including

260 Coleorrhyncha). Characters of the cephalic musculature were found that support either

261 Coleorrhyncha + Heteroptera or Coleorrhyncha + "Homoptera" (Spangenberg et al. 2013).

262   The results from recent phylogenomic analyses (Misof et al. 2014) and the present

263 wing base examination suggest that some of the above-mentioned morphological similarities

264 between Coleorrhyncha and Auchenorrhycha may be their true synapomorphies. In addition,

265 some of the features previously interpreted as synapomorphies of Coleorrhyncha and

266 Heteroptera (Schlee 1969) have already been considered as "superficial and probably not

267 significant" (Cobben 1978: but see also Schuh 1979 for critique). Based on our study, we also

268 exclude "absence of the tegula" (20-1) as a synapomorphy of Coleorrhyncha + Heteroptera.

269 This resulted in a decrease in branch support for this clade from decay index of three

270 (Friedemann et al. 2014) to only one (Fig. 4). Further morphological investigations, including

271 re-evaluation of the previously proposed synapomorphies of Coleorrhyncha and Heteroptera

272 and incorporation of these and various cephalic characters mentioned by Spangenberg et al.

273 (2013) into an explicit phylogenetic analysis, are needed to elucidate the extent of conflict

274 between morphology and phylogenomics and between different morphological character

275 systems.

276

281

282 **References**

283

284 Bourgoin T (1986a) Morphologie imaginale du tentorium des Hemiptera Fulgoromorpha. Int

285   J Ins Morph Embryo **15**:237–252.

286 Bourgoin T (1986b) Valeur morphologique de la lame maxillaire chez les Hemiptera;

287   remarques phylogénétiques. Ann Soc Entomol France (NS) **22**:413–422.

288 Bourgoin T (1993) Female genitalia in Hemiptera Fulgoromorpha, morphological and

289   phylogenetic data. Ann Soc Entomol France (NS) **29**:225–244.

290   Bourgoin T,   Huang J (1990) Morphologie comparée des genitalia mâles des

291   Trypertimorphini et remarques phylogénétiques (Hemiptera: Fulgoromoprha:

292   Tropiduchidae). Ann Soc Entomol France (NS) **26**:555–564.

293   Bourgoin T, Steffen-Campbell JD, Campbell BC (1997) Molecular phylogeny of

294   Fulgoromorpha (Insecta, Hemiptera, Archaeorrhyncha). The Enigmatic

295   Tettigometridae: Evolutionary Affiliations and Historical Biogeography. Cladistics

296   **13**:207–224.

297   Breddin G (1897) Hemipteren (Hemiptera). Ergebnisse der Hamburger magalhaensischen

298   Sammelreise, 1892/93, vol. 2. L. Friederichsen and Co., Humburg.

299   Burckhardt D (2009) Taxonomy and phylogeny of the Gondowanan moss bugs or

300   Peloridiidae (Hemiptera, Coleorrhyncha). Dtsch Entomol Ztg **56**:173–235.

301   Burckhardt D, Bochud E, Damgaard J, Bibbs GW, Hartung V, Larivière MC, Wyniger D,

302   Zürcher I (2011) A review of the moss bug genus *Xenophyes* (Hemiptera:

303   Coleorrhyncha: Peloridiidae) from New Zealand: systematics and biogeography.

304   Zootaxa **2923**:1–26.

305   Campbell BC, Steffen-Campbell JD, Sorensen JT,   Gill RJ (1995) Paraphyly of Homoptera

306   and Auchenorrhyncha inferred from 18S rDNA nucleotide sequences. Syst Entomol

307   **20**:175–194.

308   Carver M, Gross GG, Woodward TE (1991) Hemiptera (Bugs, leafhoppers, cicadas, aphids,

309   scale insects etc). In: CSIRO (ed), The Insects of Australia. 2nd edition. Cornell

310   University Press, New York, pp 429–509.

311   Cobben RH (1978) Evolutionary trends in Heteroptera Part II. Mouthpart-structures and

312   feeding strategies. Mededelingen Landbouwhogeschool Wageningen **78**(5):1–407.

313   Cryan JR, Urban JM (2012) Higher-level phylogeny of the insect order Hemiptera: is

314   Auchenorrhyncha really paraphyletic? Syst Entomol **37**:7–21.

315   Cui Y, Xie Q, Hua J, Dang K, Zou J, Liu X, Wang G, Yu X, Bu W (2013) Phylogenomics of

316   Hemiptera (Insecta: Paraneoptera) based on mitochondrial genomes. Syst Entomol

317   **38**:233–245.

318   Forero D (2008) The systematics of the Hemiptera. Rev Columbiana Entomol **34**:1–21.

319   Friedemann K, Spangenberg R, Yoshizawa K, Beutel RG (2014) Evolution of attachment

320   structure in the highly diverse Acercaria (Hexapoda). Cladistics **30**:170–201.

321   Grimaldi D, Engel MS (2005) Evolution of the Insects. Cambridge Univ. Press, Cambridge.

Hörnschemeyer T (2002) Phylogenetic significance of the wing-base of the Holometabola (Insecta). Zool Scripta **31**:17–29.

Maddison DR, Maddison WP (2001) MacClade 4: Analysis of Phylogeny and Character Evolution. Sinauer Inc., Sunderland.

Mikó I, Deans AR (2014) The second axillary in Hymenoptera. PeerJ PrePrints **2**:e428v1. http://dx.doi.org/10.7287/peerj.preprints.428v1

Misof B, Liu S, Meusemann K et al. (2014) Phylogenomics resolves the timing and pattern of insect evolution. Science **346**:763–767.

Ogawa N, Maruyama M, Yoshizawa K (2015) Wing base morphology of Aetalionidae (Hemiptera: Cicadomorpha) and its phylogenetic implications. Entomol Sci **18**:262–265.

Ouvrard D, Campbell BC, Bourgoin T, Chan KL (2000)18S rRNA secondary structure and phylogenetic position of Peloridiidae (Insecta, Hemiptera). Mol Phylog Evol **16**:403–417.

Schlee D (1969) Hennig's principles of phylogenetic systematics, and 'intuitive statisticophenetic taxonomy'? A reply to Dr. Coless' paper 'The phylogenetic fallacy'. Syst Zool **18**:127–134.

Schuh RT (1979) Review: Evolutionary Trends in Heteroptera. Part II. Mouthpart-Structure and Feeding Strategies. By R. H. Cobben. Syst Zool **28**:653–656.

Sorensen JT, Campbell BC, Gill RJ, Steffen-Campbell JD (1995) Non-monophyly of Auchenorrhyncha ("Homoptera"), based upon 18S rDNA phylogeny: Eco-evolutionary and cladistic implications within pre-Heteropterodea Hemiptera (s.l.) and a proposal for new monophyletic suborders. Pan-Pacific Entomol **71**:31–60.

Sorenson MD, Franzosa EA (2007) TreeRot, Version 3. Boston Univ., MA.

Spangenberg R, Wipfler B, Friedemann K, Pohl H, Weirauch C, Hartung V, Beutel RG (2013) The cephalic morphology of the Gondwanan key taxon *Hackeriella* (Coleorrhyncha, Hemiptera). Arthropod Struct Dev **42**:315-337.

Sweet MH (1996) Comparative external morphology of the pregenital abdomen of the Hemiptera. In: Schaefer, C.W. (ed), Studies on Hemipteran Phylogeny, Entomological Society of America, Maryland, pp 119–158.

Swofford DL (2002) PAUP*: Phylogenetic Analysis Using Parsimony (* and Other Methods), Version 4. Sinauer Inc., Sunderland.

354   Urban JM, Cryan JR (2007) Evolution of the planthoppers (Insecta: Hemiptera: Fulgoroidea).
355   Mol Phylog Evol **42**:556–572.

356   Wang Y, Chen J, Jiang LY, Qiao GX (2015) Hemipteran mitochondrial genomes: Features,
357   structures and implications for phylogeny. Int J Mol Sci **16**:12382–12404.

358   Wheeler WC, Schuh RT, Bang R (1993) Cladistic congruence among higher groups of
359   Heteroptera: congruence between morphological and molecular data sets. Entomol
360   Scandinavica **42**:121–137.

361   Yoshizawa K (2011) Monophyletic Polyneoptera recovered by wing base structure. Syst
362   Entomol **36**:377–394.

363   Yoshizawa K, Lienhard C (2016) Bridging the gap between chewing and sucking in the
364   hemipteroid insects: new insights from Cretaceous amber. Zootaxa **4079**:229–245.

365   Yoshizawa K, Saigusa T (2001) Phylogenetic analysis of paraneopteran orders (Insecta:
366   Neoptera) based on forewing base structure, with comments on monophyly of
367   Auchenorrhyncha (Hemiptera). Syst Entomol **26**:1–13.

368   Yoshizawa K, Wagatsuma M (2012) Phylogenetic relationships among superfamilies of
369   Cicadomorpha (Hemiptera: Auchenorrhyncha) inferred from the wing base structure.
370   Entomol Sci **15**:408–421.

371

372

Figure caption

Fig. 1. Forewing base structure of Coleorrhyncha. A. Line drawing, dorsal view. B. Image taken by CLSM, dorsal view. The base of the anal vein is strongly expanded and covers most of the membranous PMP (see also C). Note: the detachment between 3Ax and BA is an artifact caused by slide-mounting pressure (see A and C for their natural relationship). C. Ventral view of wing base, showing PMP region and surrounding structures. The structure in the background of the completely membranous PMP is the expanded base of the anal vein (see B for comparison).

Fig. 2. Hindwing base structure of Coleorrhyncha. A. Line drawing, dorsal view. B. Image taken by CLSM, dorsal view. Note: distortion in relative position of the notum and axillary sclerites are an artifact caused by slide-mounting pressure (see A for their natural relationship).

Fig. 3. The most parsimonious tree estimated from the wing base data (outgroups are omitted), with characters and their changes noted on the branched. A red square indicates a non-homoplasious change, and a gray triangle indicates a homoplasious change. Circled numbers are decay indices, and numbers in a square indicate bootstrap/jackknife values of adjacent branches.

Fig. 4. The strict consensus of 18 equally parsimonious trees estimated from the full morphological data set. See Fig. 3 for further explanations. Polytomies were treated as hard polytomy for character state reconstruction. Outgroups are omitted from the figure.

399   **Appendix: Characters and their state used for phylogenetic analyses.**

400

401   **Forewing base data** (modified from Yoshizawa and Saigusa 2001)

402   1. Tg: (0) present; (1) absent: $ci = 1, ri = 1$.

403   2. Tg: (0) small; (1) enlarged, with broad extention encircling the entire margin: $ci = 1, ri = 0$.

404   3. Tg: (0) with small attachment to body wall; (1) with broad attachment to body wall: $ci = 1$,

405        $ri = 0$.

406   4. HP and BSc: (0) separate from each other; (1) united with each other: $ci = 1, ri = 1$.

407   5. BSc: (0) distant from 2Ax; (1) close proximity to anteroproximal corner of 2Ax; (2) fused

408   with anteroproximal part of 2Ax: $ci = 1, ri = 1$.

409   6. BR and HP + BSc: (0) fused with each other; (1) separated from each other: $ci = 1, ri = 0$.

410   7. BR and 2Ax: (0) separate from each other; (1) fused: $ci = 0.5, ri = 0$.

411   8. 2Ax: (0) nearly flat; (1) anterior region swollen: $ci = 1, ri = 1$.

412   9. 2Ax: (0) not divided; (1) divided into two sclerites (2Ax-pp and -ad): $ci = 1, ri = 1$.

413   10. PMP: (0) located distal to 2Ax; (1) located posterodistally to 2Ax: $ci = 1, ri = 1$.

414   11. PMP: (0) nearly flat; (1) deeply concave: $ci = 1, ri = 1$.

415   12. PMP: (0) almost evenly sclerotized; (1) distal margin sclerotized more strongly than its

416   other regions: $ci = 1, ri = 1$.

417   13. PMP: (0) well sclerotized; (1) reduced, often completely membranous: $ci = 1, ri = 1$.

418   14. DMP: (0) not divided; (1) divided into 2 sclerites: $ci = 1, ri = 1$.

419   15. DMP: (0) distant from 2Ax; (1) placed next to 2Ax, articulating along a convex hinge: ci

420        $= 1, ri = 1$.

421   16. DMP: (0) large; (1) reduced in size: $ci = 1, ri = 0$.

422   17. Distal arm of 3Ax and DMP: (0) articulate with each other; (1) not articulate with each

423   other: $ci = 1, ri = 1$.

424   18. Anterior arm of 3Ax: (0) present; (1) absent: $ci = 0.5, ri = 0$.

425   19. 3Ax and BA: (0) separate from posterior margin of forewing base; (1) situated on

426   posterior margin of forewing base: $ci = 1, ri = 0$.

427   20. BA and PMP: (0) separate from each other; (1) fused with each other: $ci = 1, ri = 1$.

428

429   **Full morphology data** (modified from Friedmann et al. 2014)

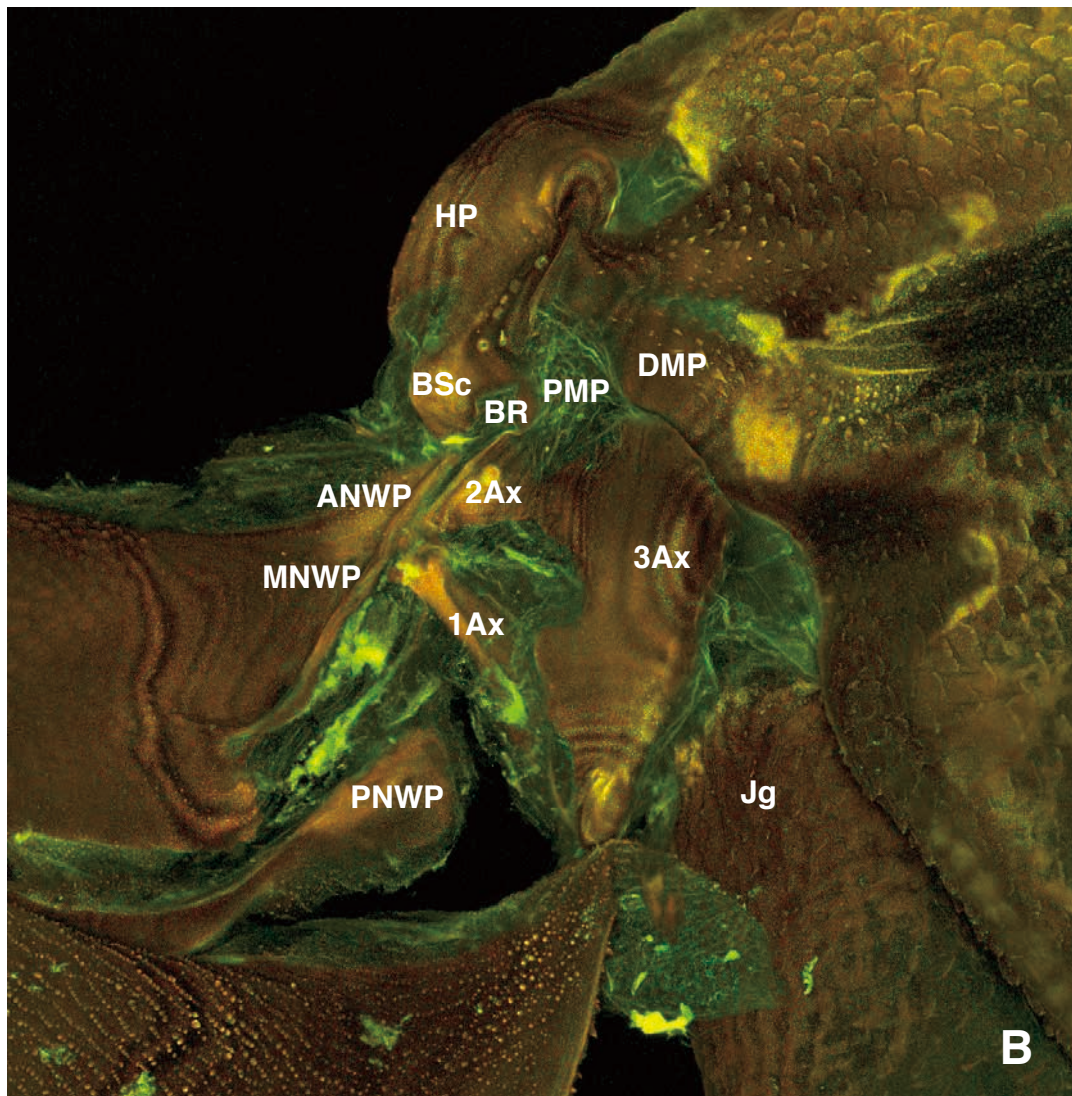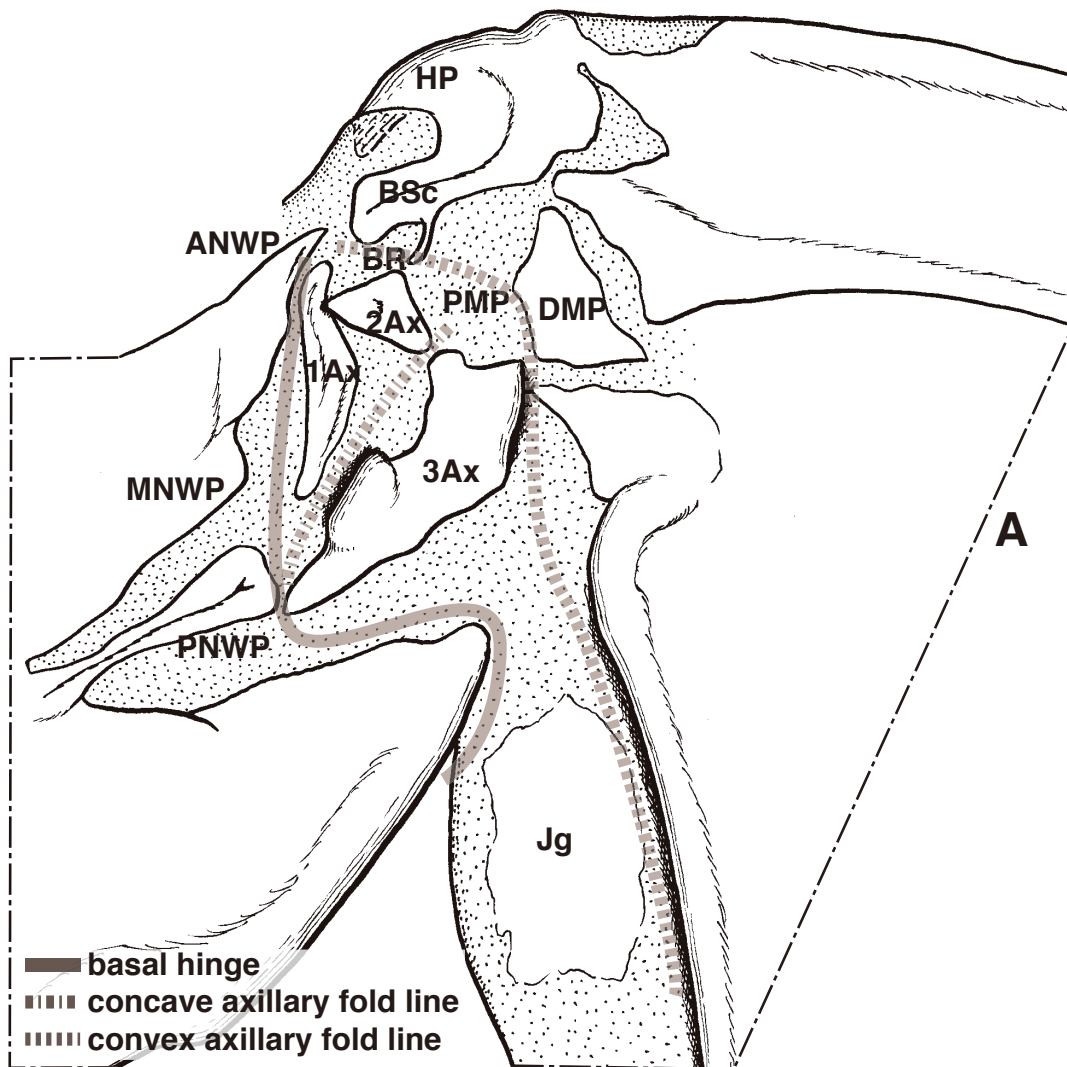430   1. Rupturing mechanism at the base of the antennal flagellum: (0) absent; (1) present: $ci = 1$,

431 ri = 1.

432 2. Exposure of mouthparts: (0) largely or completely exposed; (1) left mandible enclosed in a

433 pouch formed by anteclypeal wall, labrum, stipes, and hypopharynx; (2) bases of

434 mandibular and maxillary stylets articulate inside head with mandibular and maxillary

435 plates: $c_i = 1$, $r_i = 1$.

436 3. Right mandible: (0) present; (1) reduced: $c_i = 1$, $r_i = 0$.

437 4. Shape of mandibles: (0) not elongated; (1) elongated: $c_i = 0.5$, $r_i = 0.92$.

438 5. Cardo: (0) present; (1) strongly reduced or absent; (2) fused with stipes: $c_i = 1$, $r_i = 1$.

439 6. Lacinia: (0) absent; (1) present: $c_i = 1$, $r_i = 1$.

440 7. Insertion of lacinia: (0) on stipes; (1) detached from stipes: $c_i = 0.5$, $r_i = 0.86$.

441 8. Lacinia: (0) not elongate and stylet-like; (1) elongate and stylet-like: $c_i = 1$, $r_i = 1$.

442 9. Labial rostrum: (0) absent; (1) present: $c_i = 1$, $r_i = 1$.

443 10. Labial palps: (0) absent or strongly reduced; (1) comprising at least 2 segments: $c_i = 0.5$,

444 $r_i = 0.86$.

445 11. Cibarial water-vapour uptake apparatus: (0) absent; (1) present: $c_i = 0.5$, $r_i = 0.80$.

446 12. Jugal "bar": (0) absent; (1) present: $c_i = 1$, $r_i = 1$.

447 13. Abdominal ganglia: (0) more than two separate ganglia; (1) two separate ganglia; (2) one

448 single ganglionic mass: $c_i = 1$, $r_i = 1$.

449 14. Eyes of immature stages: (0) persist; (1) disintegrate or pulled back proximally into

450 cerebrum: $c_i = 1$, $r_i = 1$.

451 15. External wing buds: (0) present; (1) absent: $c_i = 1$, $r_i = 1$.

452 16. Pupal stage: (0) absent; (2) present: $c_i = 0.5$, $r_i = 0.5$.

453 17. Appearance of compound eyes: (0) before ultimate immature stage; (1) in ultimate

454 immature stage: $c_i = 1$, $r_i = 1$.

455 18. Ocelli of immature stages: (0) present; (1) absent: $c_i = 1$, $r_i = 1$.

456 19. Cerci of immature stages: (0) present; (1) absent: $c_i = 1$, $r_i = 1$.

457 20. Tegulae of the forewing: (0) present; (1) absent: $c_i = 1$, $r_i = 1$.

458 21. Size and shape of tegulae: (0) small; (1) enlarged, with broad extension encircling the

459 entire margin: $c_i = 1$, $r_i = 1$.

460 22. Attachment of tegulae to body wall: (0) narrow; (1) broad: $c_i = 0.5$, $r_i = 0$.

461 23. HP and BSc: (0) separated from each other; (1) connected with each other: $c_i = 1$, $r_i = 0$.

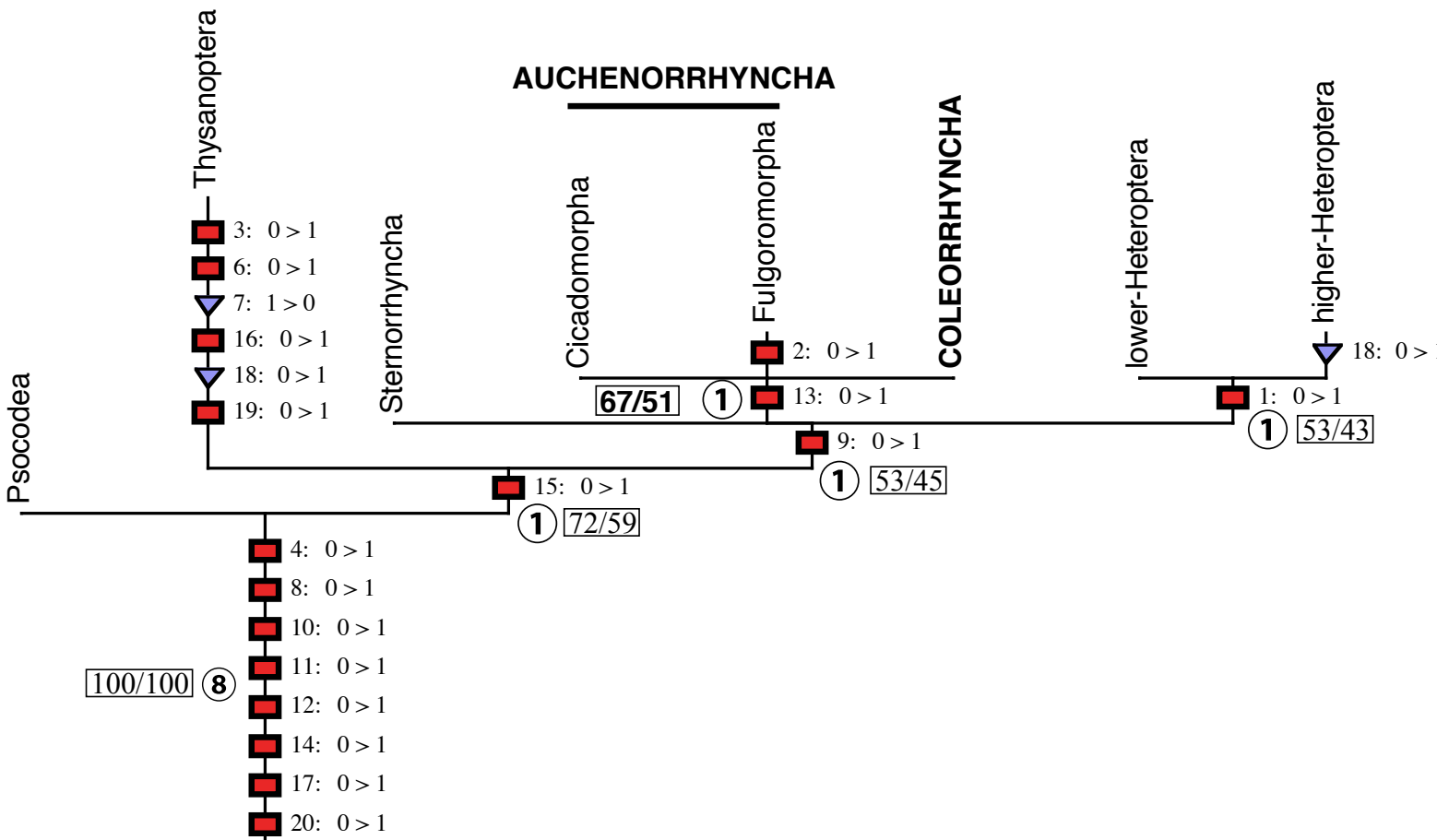462 24. BSc: (0) distant from 2Ax; (1) closely adjacent with the anteroproximal corner of 2Ax;

463 (2) fused with anteroproximal part of 2Ax: $c_i = 0.67$, $r_i = 0.67$.

464 25. BR and HP + BSc: (0) fused with each other; (1) separated from each other: $c_i = 1$, $r_i = 0$.

465 26. BR and 2Ax: (0) separated from each other; (1) fused: $c_i = 0.5$, $r_i = 0$.

466 27. 2Ax: (0) nearly flat; (1) anterior region inflated: $c_i = 1$, $r_i = 1$.

467 28. 2Ax: (0) not divided; (1) not divided: $c_i = 1$, $r_i = 1$.

468 29. Position of PMP: (0) distad 2Ax; (1) posterodistad 2Ax: $c_i = 1$, $r_i = 0$.

469 30. PMP: (0) nearly flat; (1) deeply concave: $c_i = 1$, $r_i = 0$.

470 31. PMP: (0) almost evenly sclerotized; (1) distal margin sclerotized more strongly than its
471 other regions: $c_i = 1$, $r_i = 0$.

472 32. PMP: (0) well sclerotized; (1) reduced, often completely membranous: $c_i = 0.5$, $r_i = 0.86$.

473 33. DMP: (0) not divided; (1) divided into 2 sclerites: $c_i = 1$, $r_i = 0$.

474 34. DMP: (0) distant from 2Ax; (1) placed next to 2Ax, articulating along a convex hinge: ci
475 $= 1$, $r_i = 1$.

476 35. DMP: (0) large; (1) reduced in size: $c_i = 1$, $r_i = 0$.

477 36. Distal arm of 3Ax and DMP: (0) articulating with each other; (1) not articulating with
478 each other: $c_i = 1$, $r_i = 0$.

479 37. Anterior arm of 3Ax: (0) present; (1) absent: $c_i = 0.5$, $r_i = 0$.

480 38. 3Ax and BA: (0) separate from posterior margin of forewing base; (1) attached to
481 posterior margin of forewing base: $c_i = 1$, $r_i = 0$.

482 39. BA and PMP: (0) separate from each other; (1) fused with each other: $c_i = 1$, $r_i = 0$.

483 40. Lateral hypopharyngeal arm (0) present; (1) absent: $c_i = 0.5$, $r_i = 0.88$.

484 41. Ovarioles: (0) not polytrophic; (1) polytrophic; (2) telotrophic; (3) panoistic: $c_i = 0.75$, ri
485 $= 0.92$.

486 42. Maxillary palps: (0) present, with four segments or more; (1) absent or reduced number of
487 segments: $c_i = 0.33$, $r_i = 0.8$.

488 43. Abdominal sternite 1: (0) present; (1) absent: $c_i = 0.5$, $r_i = 0.8$.

489 44. Number of axonemes in spermatozoans: (0) zero; (1) one; (2) two; (3) three: $c_i = 0.75$, ri
490 $= 0.83$.

491 45. Gonangulum: (0) not fused with tergum IX; (1) fused with tergum IX: $c_i = 0.5$, $r_i = 0.8$.

492 46. Pretentorium: (0) absent or if present not connecting internal extremities of mandibular
493 lever and corpotentorium; (1) unites internal extremities of mandibular lever and
494 corpotentorium: $c_i = 1$, $r_i = 1$.

47. Lacinial gland: (0) absent; (1) present: $c_i = 0.5$, $r_i = 0$.

48. Male genitalia: (0) symmetrical, or if asymmetrical, asymmetry not involving pregenital segments; (1) asymmetrical, this asymmetry often involving pregenital segments: $c_i = 0.5$, $r_i = 0$.

49. Accessory salivary glands generally: (0) not tubular; (1) of the tubular type: $c_i = 1$, $r_i = 0$.

50. Number of eye trichobothria of first instars: (0) one or absent; (1) two: $c_i = 1$, $r_i = 0$.

51. Number of ommatidia in first-instar larvae: (0) 4-5; (1) more than five: $c_i = 0.5$, $r_i = 0$.

52. Number of tarsomeres in first-instar larvae: (0) one; (1) two: $c_i = 1$, $r_i = 1$.

53. Forewings: (0) completely uniform or if differentiated, not forming a distinct corium-clavus and membrane; (1) forewing divided into a distinct corium-clavus and membrane: $c_i = 0.5$, $r_i = 0$.

54. Cephalic trichobothria: (0) absent in adults; (1) present in adults: $c_i = 1$, $r_i = 1$.

55. Metathoracic scent gland system: (0) absent; (1) present: $c_i = 1$, $r_i = 1$.

56. Labium: (0) not tubular; (1) tubular labium with three segments; (2) tubular labium with four segments: $c_i = 1$, $r_i = 1$.

57. Insertion of tubular labium: (0) posteriorly on the head, (1) anteriorly on the head: $c_i = 1$, $r_i = 1$.

58. Dorsal abdominal glands in immature stages: (0) absent; (1) present: $c_i = 1$, $r_i = 1$.

59. Number of antennal flagellomeres: (0) more than 4, (1) 4 or less: $c_i = 0.33$, $r_i = 0.75$.

60. Articulations between the mesomere, anterodorsal extension of ventral plate and posterior end of basal plate: (0) absent; (1) present: $c_i = 0.5$, $r_i = 0.5$.

61. Length of basal apodeme of the phallic organ: (0) short; (1) long, longer than basal plate: $c_i = 1$, $r_i = 0$.

62. Third posterodorsal corner of basal plate: (0) not extended; (1) extended posteriorly: $c_i = 1$, $r_i = 0$.

63. Basal apodeme of the phallic organ: (0) present; (1) absent: $c_i = 1$, $r_i = 1$.

64. Width of basal apodeme: (0) narrow; (1) as broad as or broader than basal plate: $c_i = 1$, $r_i = 1$.

65. Ventral plates 1: (0) separated; (1) partly fused anteriorly: $c_i = 1$, $r_i = 1$.

66. Ventral plates 2: (0) separated or partly fused; (1) completely fused: $c_i = 1$, $r_i = 0$.

67. Mesomere of the aedeagus: (0) rounded posteriorly; (1) pointed posteriorly: $c_i = 0.5$, $r_i = 0.5$.
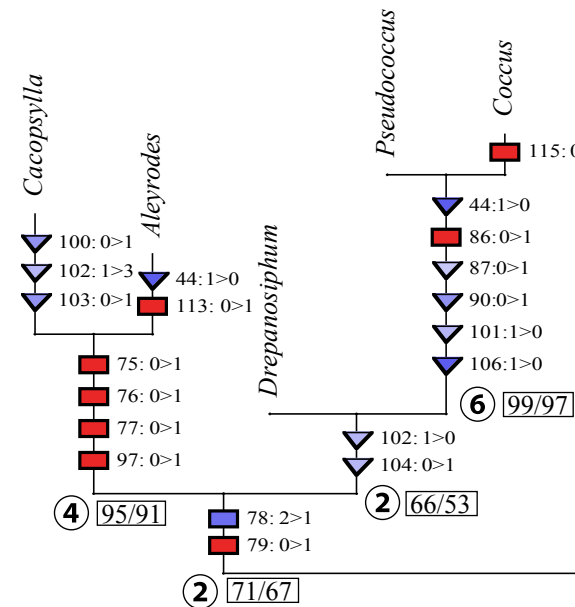
527   68. Posteromedian part of basal plate: (0) membranous; (1) sclerotized: $c_i = 1$, $r_i = 1$.

528   69. Anterior end of mesomere: (0) articulated with basal plate; (1) articulated with paramere:

529        $c_i = 1$, $r_i = 0$.

530   70. Paired ocelli in nymphs or larvae: (0) absent; (1) present: $c_i = 1$, $r_i = 1$.

531   71. Intrinsic antennal muscles (Mm. scapopedicellares) in immature stages: (0) absent; (1)

532   present: $c_i = 1$, $r_i = 1$.

533   72. Ventral metasternal process: (0) absent; (1) present: $c_i = 1$, $r_i = 1$.

534   73. Sensory plate organs of pedicel: (0) absent; (1) present: $c_i = 1$, $r_i = 1$.

535   74. Evan's organ: (0) absent, (1) present: $c_i = 0.5$, $r_i = 0.86$.

536   75. Ductus ejaculatorius: (0) normal; (1) modified as a sperm pump: $c_i = 1$, $r_i = 1$.

537   76. Proximal abdomen pediculate by reduction of the 1st and 2nd segment: (0) absent; (1)

538   present: $c_i = 1$, $r_i = 1$.

539   77. Hind coxae: (0) normally developed; (1) broad, closely adjacent: $c_i = 1$, $r_i = 1$.

540   78. Proboscis: (0) absent; (1) shifted posteriorly between bases of procoxae; (2) not shifted

541   posteriorly between bases of procoxae: $c_i = 0.67$, $r_i = 0.94$.

542   79. Posterior parts of the head capsule: (0) sclerotized; (1) membraneous: $c_i = 1$, $r_i = 1$.

543   80. Connective tissue occluding occipital foramen: (0) absent; (1) present: $c_i = 0.5$, $r_i = 0$.

544   81. Ovipositor simplified: (0) absent; (1) present: $c_i = 0.5$, $r_i = 0.5$.

545   82. Spiracular glands: (0) absent; (1) present: $c_i = 0.5$, $r_i = 0$.

546   83. Extension of the occipital apodeme reaching into the thorax: (0) absent; (1) present: $c_i =$

547   0.5, $r_i = 0$.

548   84. Pronotum and procoxae: (0) not fused; (1) fused: $c_i = 1$, $r_i = 1$.

549   85. Position of anterior tentorial pits: (0) frontal side of head; (1) absent; (2) shifted dorsally:

550        $c_i = 1$, $r_i = 1$.

551   86. Fusion of head and thorax: (0) absent; (1) present: $c_i = 1$, $r_i = 1$.

552   87. Body and head: (0) not flattened; (1) dorsoventrally flattened: $c_i = 0.25$, $r_i = 0.67$.

553   88. Hind femora: (0) not enlarged; (1) enlarged: $c_i = 0.33$, $r_i = 0.6$.

554   89. Meso- and metanotum: (0) not fused; (1) fused: $c_i = 1$, $r_i = 1$.

555   90. Compound eyes: (0) not reduced; (1) only 2 ommatidia or less: $c_i = 0.5$, $r_i = 0.86$.

556   91. Labial palp: (0) present; (1) absent: $c_i = 0.5$, $r_i = 0.88$.

557   92. Complex tymbal acoustic system: absent (0); present (1): $c_i = 1$, $r_i = 1$.

558   93. Aristate antennal flagellum: (0) absent; (1) present: $c_i = 0.5$, $r_i = 0.86$.

559 94. Malpighian tubules: (0) more than six; (1) six; (2) four or less: $c_i = 1$, $r_i = 1$.

560 95. Labrum: (0) not narrowed; (1) narrowed: $c_i = 1$, $r_i = 1$.

561 96. Mandibular and lacinial stylets: (1) unicondylar; (0) dicondylar: $c_i = 1$, $r_i = 1$.

562 97. Pedunculate eggs (with stalk): (0) absent; (1) present: $c_i = 1$, $r_i = 1$.

563 98. Gut with filter chamber containing Malpighian tubules: (0) absent; (1) present: $c_i = 1$, $r_i =$
564   1.

565 99. Coronal (= median epicranial) suture: (0) absent; (1) present: $c_i = 0.33$, $r_i = 0.33$.

566 100. Parempodia on unguitractor plate: (0) absent; (1) elongate and setiform, inserted in an
567   alveolus: $c_i = 0.5$, $r_i = 0.5$.

568 101. Number of tarsal segments: (0) one; (1) two; (2) three; (3) more than three. State 3 is
569   adopted for Mydiognathus: $c_i = 0.33$, $r_i = 0.65$.

570 102. Arolium: (0) absent; (1) present; (2) eversible; (3) bilobed: $c_i = 0.33$, $r_i = 0.45$.

571 103. Sticky terminal lip of arolium: (0) absent; (1) present: $c_i = 0.5$, $r_i = 0.67$.

572 104. Pulvilli: (0) absent; (1) present: $c_i = 0.33$, $r_i = 0.6$.

573 105. Euplantulae: (0) absent, (1) present: $c_i = 0.33$, $r_i = 0.33$.

574 106. Number of claws: (0) one; (1) two; (2) reduced into spoon-shaped plates; (3) main claw
575   plus accessory claw: $c_i = 0.75$, $r_i = 0.67$.

576 107. Claw teeth: (0) absent; (1) present: $c_i = 0.33$, $r_i = 0.33$.

577 108. Protuberance with microtrichia on distolateral side of the pretarsus: (0) absent; (1)
578   present: $c_i = 1$, $r_i = 0$.

579 109. Sensorial setae on mesal side of arolium: (0) absent; (1) present: $c_i = 1$, $r_i = 1$.

580 110. Adhesive claw setae: (0) absent; (1) present: $c_i = 1$, $r_i = 0$.

581 111. Eversible structure between tibia and tarsus: (0) absent; (1) present: $c_i = 0$, $r_i = 0$.

582 112. Tibial thumb-like process: (0) absent; (1) present: $c_i = 1$, $r_i = 0$.

583 113. Empodial paronychium: (0) absent; (1) present: $c_i = 1$, $r_i = 0$.

584 114. Tarsal apophysis on the ventral side of the tarsus: (0) absent; (1) present: $c_i = 1$, $r_i = 0$.

585 115. Two dorsal capitate setae: (0) absent; (1) present: $c_i = 1$, $r_i = 0$.

586 116. Flag-like sensilla on the 1st tarsal segment: (0) absent; (1) present: $c_i = 1$, $r_i = 0$.

587 117. Fingerlike process below claw: (0) absent; (1) present: $c_i = 1$, $r_i = 0$.

588 118. Ventral brush: (0) absent; (1) present: $c_i = 0.5$, $r_i = 0$.

A

C

B

Thysanoptera

Psocodea

AUCHENORRHYNCHA

COLEORRHYNCHA

Cicadomorpha

Fulgoromorpha

Sternorrhyncha

lower-Heteroptera

higher-Heteroptera

3: 0 > 1
6: 0 > 1
7: 1 > 0
16: 0 > 1
18: 0 > 1
19: 0 > 1

2: 0 > 1
13: 0 > 1

18: 0 > 1
1: 0 > 1

67/51 ①

9: 0 > 1
① 53/45

① 53/43

15: 0 > 1
① 72/59

4: 0 > 1
8: 0 > 1
10: 0 > 1
11: 0 > 1
12: 0 > 1
14: 0 > 1
17: 0 > 1
20: 0 > 1

100/100 ⑧

STERNORRHYNCHA

Cacopsylla

Aleyrodes

Pseudococcus

Coccus

115: 0>1

100: 0>1
102: 1>3
103: 0>1

44: 1>0
113: 0>1

Drepanosiphum

44:1>0
86: 0>1
87:0>1
90:0>1
101:1>0
106:1>0

(6) | 99/97

75: 0>1
76: 0>1
77: 0>1
97: 0>1

102: 1>0
104: 0>1

(4) | 95/91

(2) | 66/53

78: 2>1
79: 0>1

(2) | 71/67

AUCHENORRHYNCHA

Cixius

Javasella

Dictyophara

Philaenus

Cicadetta

Centrotus

Cicadella

21: 0>1
46: 0>1
73: 0>1

103: 0>1

108: 0>1   102:1>0

102:1>3
109: 0>1

(1) | 80/71

98: 0>1

(4) | 99/92

(1) | 60/51

32: 0>1
74: 0>1
92: 0>1
93:0>1
101: 1>2

(3) | 94/88

5: 0>1
9: 0>1
28:0>1
56:0>1

(3) | 88/85

COLEORRHYNCHA

HETEROPTERA

Graphosoma

Systelloderes

Ceratocombus

37:0>1
49:0>1
101:1>2
104:0>1

50:1>0

48:0>1

24:2>1
32:0>1
74:0>1
87:0>1

20: 0>1
52:1>0
55: 0>1
57: 0>1
58: 0>1
100:0>1
102:1>0

(6) | 100/99

54: 0>1
56:1>2
59:0>1

(1) | **52/47**